Journal of New Materials for Electrochemical Systems 18, 131-135 (2015)

Effects of Nano Carbon Conductive Additives on the Electrochemical Performance of $LiCoO_2$ Cathode for Lithium Ion Batteries

Xinlu Li*, Xinlin Zhang, Tongtao Li, Qineng Zhong, Yanyan Zhang and Jiamu Huang

School of Materials Science and Engineering, Chongqing University, Chongqing, 400030, P. R. China

Received: March 21, 2015, Accepted: April 21, 2015, Available online: September 28, 2015

Abstract: *Carbon black(CB), multi-walled carbon nanotubes(CNTs) and graphene nanosheets(GNs) were employed as carbon conductive additives for $LiCoO_2$(LCO). X-ray diffraction, transmission electron microscopy and scanning electron microscopy were used to characterize the crystal structure and morphology of samples. And the specific surface area and porosity structure of the three kinds of carbon conductive additives were measured by N_2 adsorption-desorption. To investigate the effect on the electrochemical reaction activity, galvanostatic discharge-charge experiments showed that the composite of LCO-GNs exhibited the highest specific capacity of 167mAh/g at 0.1C and 123 mAh/g at 1 C rate. The flexible wrapping of GNs and bridging nearby LCO particles together were found to enhance electrical conductivity most effectively.*

Keywords: $LiCoO_2$; Carbon conductive additives; Graphene nanosheets; Lithium-ion batteries

1. INTRODUCTION

Electrochemical energy storage has become an increasingly important research area in recent years [1]. Lithium-ion batteries (LIBs) have been considered as potential power sources for portable electronic devices, hybrid electric vehicles and grid energy storage with high energy density, high safety, low cost and environmental benign [2-4]. $LiCoO_2$, $LiNiO_2$ and $LiMn_2O_4$ have served as very effective cathode active materials in lithium ion batteries [5-7].Among them, layer structured $LiCoO_2$ is still considered the most important commercial cathode material for LIBs owing to its high voltage, high reversible capacity and long cycle stability[8].Moreover, charging of the layered Li_xCoO_2 material from $LiCoO_2$ to $Li_{0.5}CoO_{1.5}$ resulted in large anisotropic volume change of the host lattice in the c-axis direction as large as 7%[9].Such volume change caused serious polarization and poor utilization of active materials.

In order to make full use of the active materials and increase the capacity, conductive additives were used to provide conductive path from the current collector to the active material through the electrode [10]. Carbonaceous materials, such as carbon black, graphite and carbon nanotubes, were widely used as conductive additives due to their high electrical conductivity [11-16]. Cheon et al[17] reported that the $LiCoO_2$ cathode with a binary conductive at an appropriate weight ratio (LCO) Lonza KS6 to Super-P had a better cycle life than that with a single conductive additives. Park et al. [18] also found that $LiCoO_2$ mixing with 8 wt% CNTs exhibited a high discharge capacity of 136 mAh/g at 5 C rate and a capacity retention of 97% for 50 cycles at 1 C rate. Graphene, a two-dimensional aromatic monolayer of carbon atom, is an alternative of conductive carbon with superior electrical conductivity, a high specific surface area, and structural flexibility[19-20]. However, less effort was put on graphene nanosheets(GNs) as conductive additives in LCO according to previous reports.

In this work, three kinds of carbon additives in different dimensions (CB,CNTs and GNs) are added in $LiCoO_2$ cathode materials to construct different networks. The illustration of LCO-CB, LCO-CNTs and LCO-GNs composite was presented in Fig .1. We also discuss the effect of three kinds of carbon additives on improvement in conductivity and electrochemical performance of $LiCoO_2$.

2. EXPERIMENTAL

2.1. Materials Preparation

All reagents were of analytical grade. The $LiCoO_2$ particles (D_{50}=6.55μm, JIANGMEN KANHOO INDUSTRY CO. LTD) were used as the cathode active material. Carbon black (OD=50nm) were purchased from JingRui Battery Co. Ltd.

*To whom correspondence should be addressed: Email: lixinlu@cqu.edu.cn
Phone: +86-23-65127940; Fax: +86-23-65127306

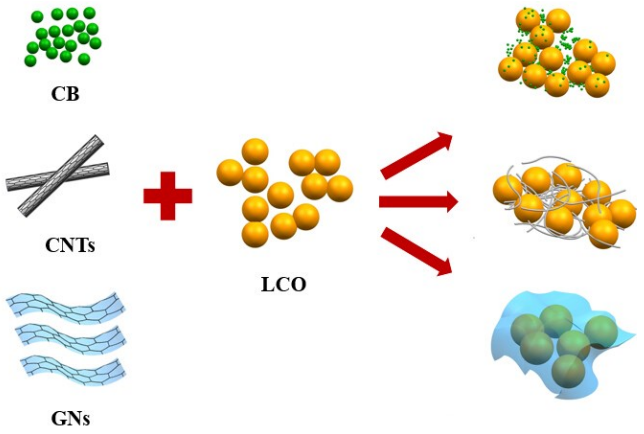

Figure 1. Schematic illustration of the LCO-CB, LCO-CNTs and LCO-GNs.

(Guangzhou, China). Carbon nanotubes (CNTs, OD=30-50nm, Length=10-20μm) were purchased from Timesnano, (Chengdu Organic Chemicals Co. Ltd., Chinese Academy of Sciences). Graphite oxides (GO) were prepared from natural flake graphite (10 mesh, Alfa Aesar) by a modified Hummers' method. Briefly, graphite (3.0 g) was added to concentrated sulfuric acid (100 mL) with vigorous stirring in an ice bath. Then, 3g $NaNO_3$ and 15 g $KMnO_4$ were slowly added to the above mixture in the continuous stirring for another 4 h. Then, the suspension was transferred to a 35-40°C water bath for about 12 h. After that, 400 mL of deionized water and 5 mL of H_2O_2 (30 wt %) were added to the mixture. The product was obtained after filtration. The solid residue was washed with dilute HCl aqueous solution and distilled water until the filtration was neutral. Then the GO were obtained after drying at 60℃ for 12h. Finally, rapid heating at 2000℃/min for 10s to split the GO into individual sheets, then GNs were obtained.

2.2. Microstructure characterization

The crystal structure was characterized by X-ray diffraction (XRD, DMAX-2500PC, Cu Kα radiation, λ=1.5406 Å). The morphology of samples were observed using scanning electron microscope (SEM, FEI Nova 400, Zeiss Auriga FIB) and high-resolution transmission electron microscope (HRTEM, LIBRA 200 FE at 200 kV). The Brunauer-Emmett-Teller (BET) surface area and pore structure were analyzed by N_2 adsorption-desorption using Micrometrics ASAP 2020.

2.3. Electrochemical measurement

The working electrodes were prepared of 80 wt.% $LiCoO_2$, 10 wt.% conductive additives (CB, CNTs, GNs, respectively), and 10 wt.% of polyvinylidene difluoride in N-methyl-2-pyrrolidone to form a slurry. Then the slurry was uniformly pasted on Al foil substrates. The foils were dried at 80°C for 4h, then we prepared Φ16mm foils under 15 MPa gas-pressure. The working electrode was dried in vacuum oven at 120 °C for 24 h before assembling cells. Electrochemical tests was performed by assembling a two-electrode configuration by CR2430 coin cells in an argon-filled glove box, in which a lithium-metal foil was used as the corresponding electrode and porous polyethylene separator (Celgard 2400) as the membrane. 1 M $LiPF_6$ in the volume ratio of 1:1 ethyl methyl carbon (EMC)-dimethyl carbonate (DMC) as the electrolyte. Electrochemical impedance spectroscopy (EIS) and cyclic voltammetry(CV) were carried out using Solartron (1260 + 1287). CV was tested in the potential window of 3.00 V-4.25V at a scanning rate of 0.05mV/s And galvanostatic discharge-charge cycles were conducted on a battery test system (Arbin BT 2000) at different current densities between 3.00V and 4.25V.

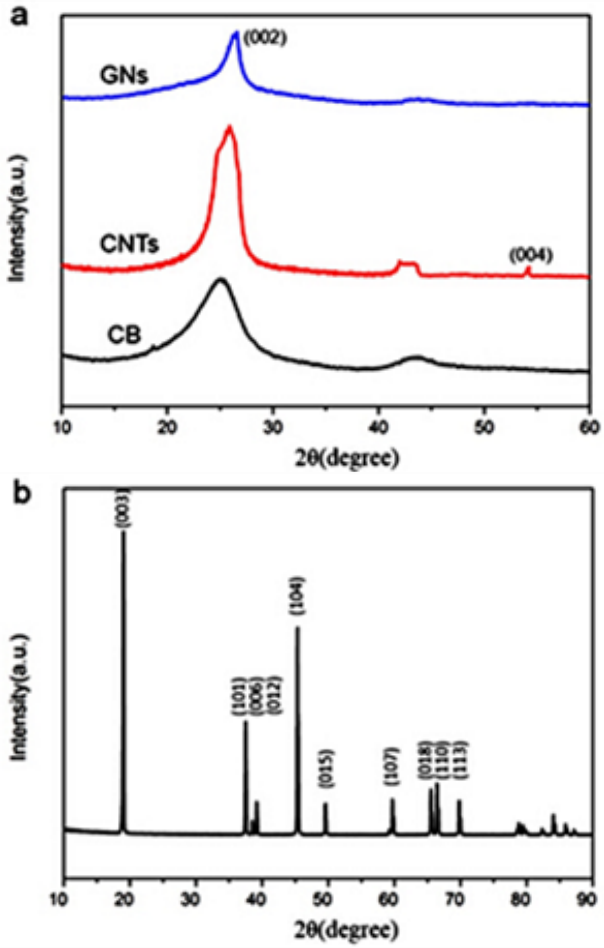

Figure 2. XRD patterns of (a) carbon conductive additives and (b) $LiCoO_2$.

3. RESULTS AND DISCUSSION

XRD patterns of CB, CNTs and GNs are presented in Fig.2(a).Compared with CNTs, GNs and CB exhibit broader peak and lower intensity at the peak of (002) plane. Moreover, the interlayer spacing d (002) of GNs(0.356nm) is larger than graphite, which is attributed to the expansion of graphite oxides between graphene layers during the heat treatment at 2000ºC. The sharpest (002) peak and the most distinct (004) peak in the XRD pattern of CNTs proved that the CNTs show the highest degree of graphitization among the three conductive additives. Fig. 2(b) shows the XRD pattern of $LiCoO_2$, all the diffraction peaks are in good agree-

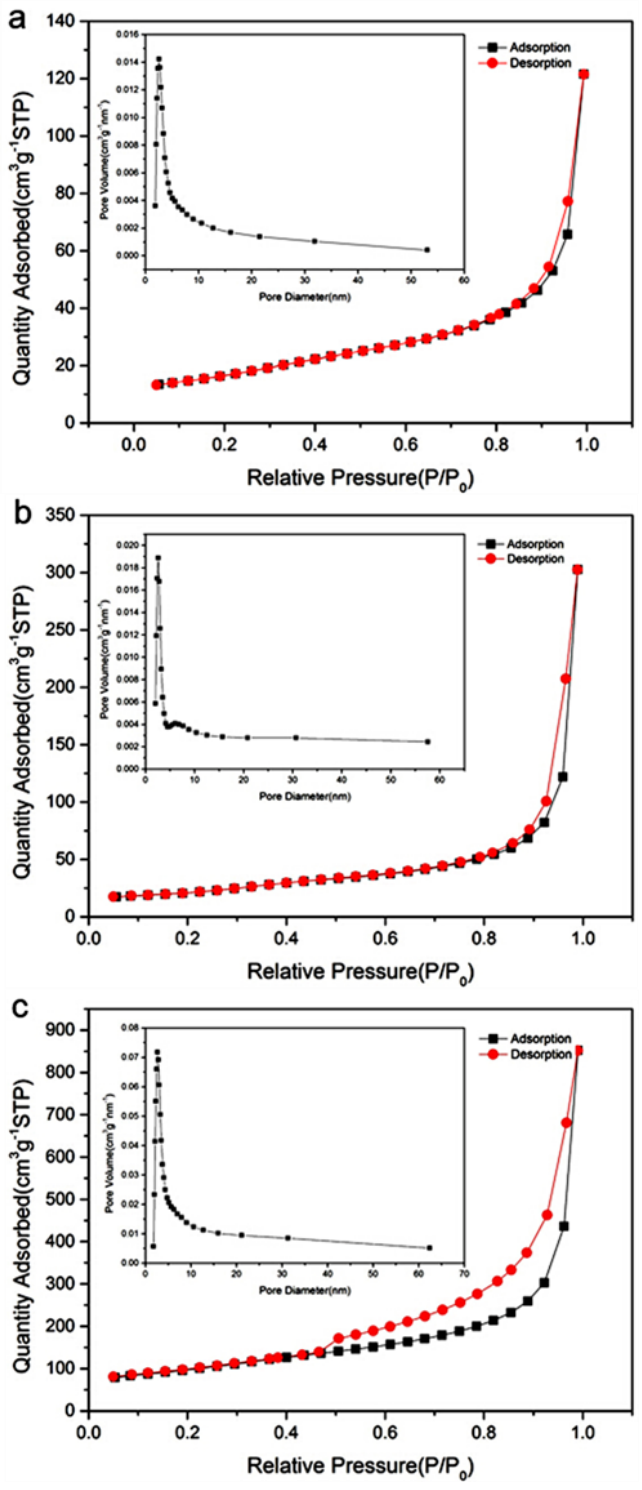

Figure 3. Nitrogen adsorption/desorption isotherms and pore size distribution (inset) of CB (a), CNTs (b) and GNs (c)

ment with the standard profiles of $LiCoO_2$ (JCPDS No. 50-0653), and no peaks of impurity are found.

Nitrogen adsorption/desorption isotherms and pore size distribution of CB, CNTs and GNs are compared in Fig. 3. CB, CNTs and GNs exhibit the Type IV adsorption isotherms with the Type H3 hysteresis loop, indicating the cylinder-shaped pores on the surface. The BET specific surface area of GNs (341.9m^2/g) is higher than that of CB (59.4 m^2/g) and CNTs (75.2 m^2/g). The large surface of GNs can absorb more electrolytes solution and then provide sufficient lithium ions to buffer for quick electrochemical reactions.

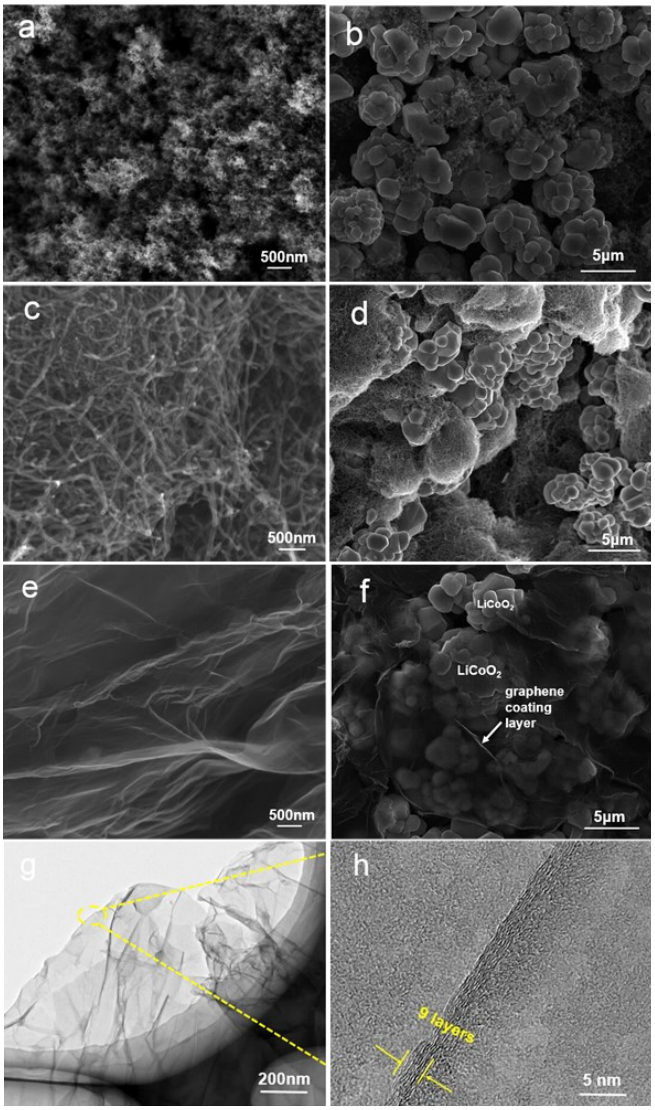

Figure 4. FESEM images of (a)CB, (b)LCO-CB, (c)CNTs, (d)LCO-CNTs, (e)GNs, (f)LCO-GNs. HRTEM images of GNs(g) and (h).

Fig. 4 shows the SEM images of $LiCoO_2$ mixing with three different carbon conductive additives. As shown in Fig. 4(b), $LiCoO_2$ were surrounded by CB nanoparticles randomly. CB nanoparticles easily accumulate in the interspace among $LiCoO_2$, and it is very difficult for CB particles to link up with each other to form a continuous network on the surface of $LiCoO_2$. Fig. 4(d) shows the SEM image of $LiCoO_2$ with CNTs. Obviously, CNTs can form a continuous network, however, they tend to agglomerate so serious-

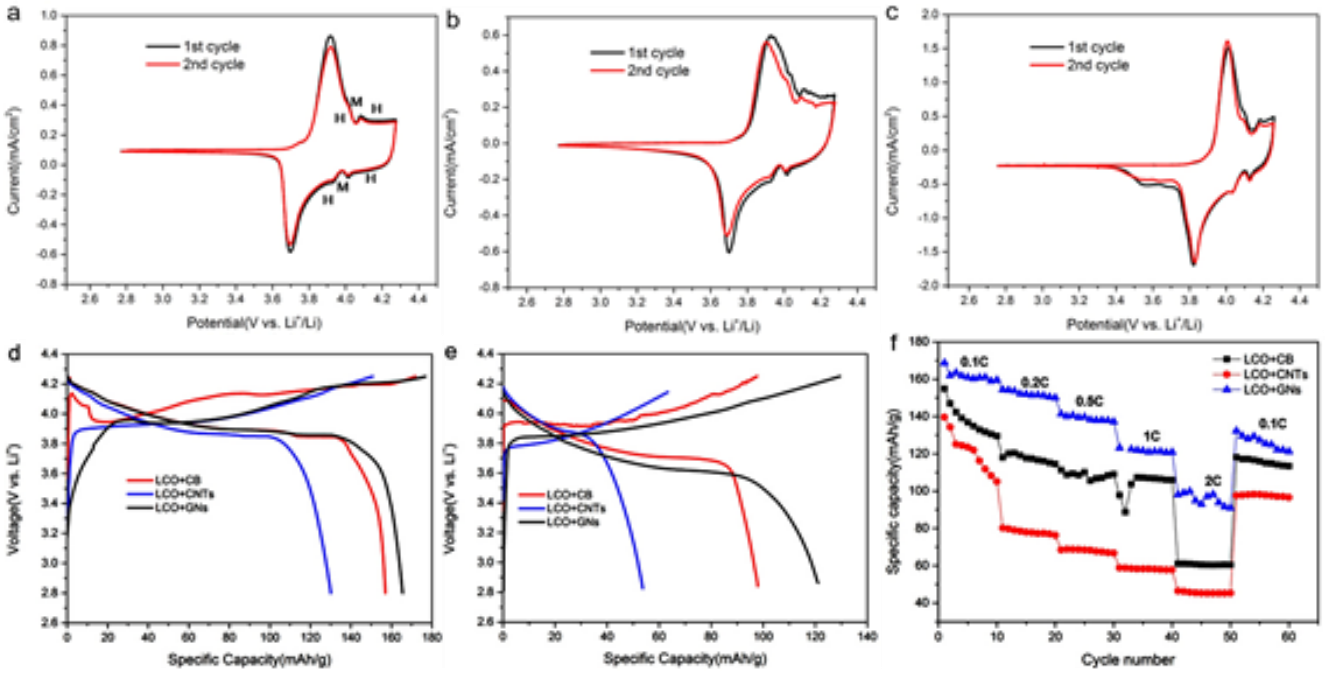

Figure 5. CV curves for the first 2 cycles of (a) LCO-CB, (b) LCO-CNTs, (c) LCO-GNs, the first charge-discharge curves at 0.1C(d) and 1C(e), (f) rate performance of LCO-CB,LCO-CNTs and LCO-GNs.

ly that they cannot contact with $LiCoO_2$ particles intimately. GNs can be easily identified as the thin and flexible sheets that ''wrap'' $LiCoO_2$ particles closely and also cover nearby particles together as shown in Fig. 4(f), which can remarkably increase the contacted area between $LiCoO_2$ and GNs. HRTEM images of GNs are showed in Fig. 4(g) and (h) to further verify the microstructure of the GNs. The GNs are composed of 9 graphene layers.

Fig. 5(a), (b) and (c) show the cyclic voltammograms for $LiCoO_2$ mixing with CB, CNTs and GNs respectively. The symbols H and M represent hexagonal and monoclinic phases, respectively [21]. All redox peaks in the cyclic voltammograms are mainly due to phase transitions during the topotactic reactions. And the order-to-disorder transition of lithium ions in the CoO_2 framework leads to the Li^+ intercalations [22, 23]. For LCO-GNs, the oxidation and reduction peaks in the second cycle appear at around 4.00V and 3.83V. The potential interval (0.17V) between two redox peaks of LCO-GNs is smaller than that of LCO-CB (0.22 V) and LCO-CNTs (0.20V), which is attributed to the improved reaction activity of LCO-GNs. The first charge-discharge curves at 0.1 C are presented in Fig. 5(d). It can be clearly observed that all the three electrodes had irreversible capacity loss in the first cycle. LCO-GNs is able to deliver the highest charge capacities (167mAh/g) among LCO-CB,LCO-CNTs and LCO-GNs. Flexible GNs wrap the $LiCoO_2$ particles closely to form a continuous conductive network and enhance the electronic conductivity most effectively among the three carbon conductive additives. Moreover, the porous GNs also facilitate more Li^+ insertion/desertion. The first discharge and charge capacities of LCO-CNTs are the lowest, which is due to the agglomeration of CNTs that cannot form continuous conductive path well. The galvanostatic discharging voltage profiles at 1C rate is shown in Fig. 5(e).The difference between the charge capacity

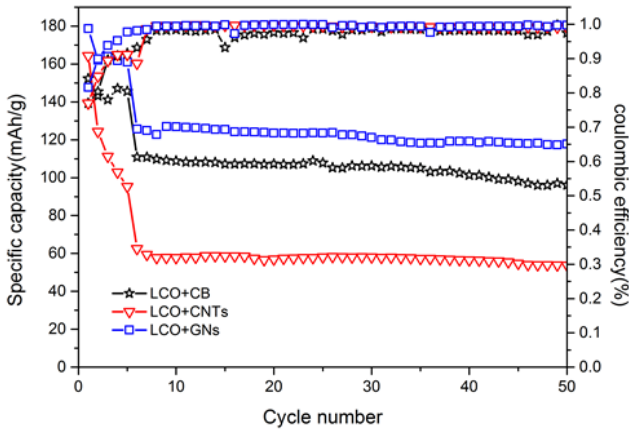

Figure 6. Cycling performances of LCO-CB, LCO-CNTs and LCO-GNs at 1 C.

and discharge capacity of LCO-GNs is the smallest, in other words, LCO-GNs possess the highest coulombic efficiency, which is due to the most contacted area enhance the electrochemical reaction activity.

Fig. 5(f) shows the rate capability of LCO-CB, LCO-CNTs and LCO-GNs. LCO-GNs exhibits the highest specific capacity of 167mAh/g at 0.1C and 123 mAh/g at 1 C, which can be ascribed to the best electrochemical reaction activity. Besides, the porous structure of GNs also facilitates Li^+ insertion/desertion. However, the specific capacity of LCO-CB is 158 mAh/g at 0.1 C and 97 mAh/g at 1 C, and LCO-CNTs delivers a lower capacity of 125mAh/g and 59 mAh/g at the same rate.

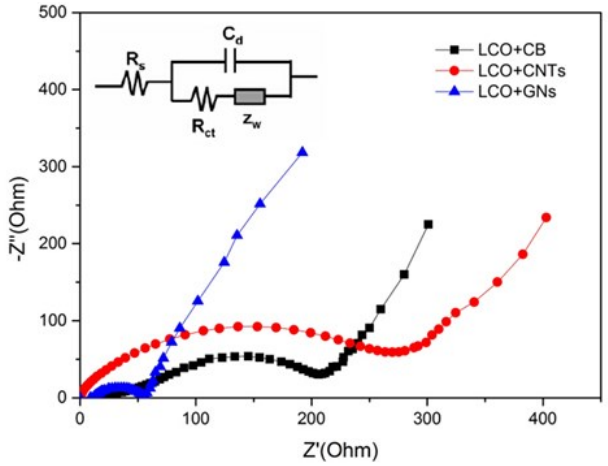

Figure 7. EIS Nyquist plots of LCO-CB, LCO-CNTs, LCO-GNs in the frequency ranges from 100 kHz to 0.1 Hz.

The cycling performance of LCO-CB, LCO-CNTs and LCO-GNs at 1C is illustrated in Fig. 6. Obviously, LCO-CB, LCO-CNTs and LCO-GNs exhibit excellent performance at 1C. The coulombic efficiency of LCO-GNs rapidly change from 81.5% to 93.2% in the first three cycles and then maintain about 99% in the following cycles. Moreover, after 50 cycles at 1 C, it still remains a high reversible capacity of 117 mAh /g with a capacity retention of 67%.

Electrochemical impedance measurement was carried out to investigate the electrochemical property of the three kinds of nanocomposites. The high-frequency arc is referred to the solid electrolyte interphase resistance (R_f), The semicircle in the high and middle frequency range represented the charge-transfer resistance (R_{ct}) on electrode–electrolyte interface, and the inclined line at lower frequency represents the Warburg impedance (Z_W) associated with the lithium-diffusion in the in the solid phase of $LiCoO_2$ and carbon materials [5]. LCO-GNs showed the lowest charge transfer resistance, proving the highest electron conductivity, which can be attributed to the intimate and large contact between $LiCoO_2$ and GNs. Meanwhile, there are more pore volume with the pore width less than 50 nm in the case of LCO-GNs (as showed in Fig. 3(c)), which can facilitate the penetration of electrolytes and transport of solvented Li^+[24].

4. CONCLUSIONS

Compared to CB and CNTs, flexible and porous GNs wrap the $LiCoO_2$ particles closely to form a continuous conductive network and facilitate electron removal. Discontinuous network, inhomogeneous distribution and loose contact of CB or CNTs will decrease the electrochemical performance of cathode active materials. GNs are found to be the most effective carbon conductive additives in improving the electrochemical reaction activity of the cathode active materials for lithium batteries.

5. ACKNOWLEDGEMENTS

The authors are grateful for the financial support from the Project No. CDJZR13130027 of the Fundamental Research Funds for the Central Universities and National Natural Science Foundation of China (No.51172293) and the technical support from the Laboratory of Advanced Carbon Functional Nanomaterials (Chongqing University, China).

REFERENCES

[1] K. H. Seng, G. D. Du, L. Li, Z. X. Chen, H. K. Liu, Z. P. Guo. Journal of Materials Chemistry, 22, 16072 (2012).
[2] Y. Wang, G. Cao, Advanced Materials, 20, 2251 (2008).
[3] A. K. Geim, Nature materials, 4,805 (2005).
[4] K. Saravanan, K. Ananthanarayanan, P. Balaya, Energy & Environmental Science, 3, 939 (2010).
[5] J. H. Lee, J. K. Hong, D. H. Jang, Journal of power sources, 89, 7 (2000).
[6] J. Shirakawa, M. Nakayama, H. Ikuta, Electrochemical and solid-state letters, 7, A27 (2004).
[7] C. A. Frysz, X. P. Shui, D.D.L. Chung, Journal of power sources, 58, 41 (1996).
[8] T. Wei, R. Zeng, Y. M. Sun, CHEMICAL COMMUNICATIONS , 50, 1962 (2014).
[9] T. Motohashi , Y. Katsumata , T. Ono , R. Kanno , M. Karppinen , H. Yamauchi,
Chemistry of Materials, 19, 5063 (2007).
[10]U. Dettlaff-Weglikowska, J. Yoshida, N. Sato, S. Roth, Journal of The Electrochemical Society, 158, A174 (2011).
[11]J. S. Sakamoto, B. Dunn, Journal of the Electrochemical Society, 149, A26 (2002).
[12]Q. Lin, J. N. Harb, Journal of The Electrochemical Society, 151, A1115 (2004).
[13]J. K. Hong, J. H. Lee, S. M. Oh, Journal of power sources, 111, 90 (2002).
[14]S. Mandal, J. M. Amarilla, J. Ibáñez, J. M. Rojo, Journal of the Electrochemical Society, 148, A24 (2001).
[15]J. Lahaye, M. J. Wetterwald, J. Messiet,Journal of applied electrochemistry, 14, 117 (1984).
[16]L Fransson, T Eriksson, K Edström, T Gustafsson, J.O Thomas, Journal of power sources, 101,1 (2001).
[17]S.E. Cheon, C.W. Kwon, D.B. Kim, S.J. Hong, H.T. Kim, S.W. Kim, Electrochimica acta, 46, 599 (2000).
[18]J. H. Park, S.Y. Lee, J. H. Kim, S. Ahn, J. S. Park, Y. U. Jeong, Journal of Solid State Electrochemistry, 14, 593 (2010).
[19]C. Zhang, X. Peng, Z. Guo, Carbon, 50, 1897 (2012).
[20]C. M. Chen , Q. Zhang, M. G. Yang, Carbon, 50, 3572 (2012).
[21]J Cho, Y. J. Kim, B. Park, Journal of the Electrochemical Society, 148, A1110 (2001).
[22]K. Dokko, M. Mohamedi, Y. Fujita, T. Itoh, M. Nishizawa, M. Umeda, I. Uchida, Journal of the Electrochemical Society, 148, A422 (2001).
[23]E.I Santiago, A.V.C Andrade, C.O Paiva-Santos, L.O.S Bulhões, Solid State Ionics, 158,91 (2003).
[24]X. Liu, M. H. Wu, M. R. Li, X. L. Pan, Journal of Materials Chemistry A, 1, 9527 (2013).